

GPI Control for a Single-Link Flexible Manipulator

J. Becedas*, V. Feliu * and H. Sira-Ramírez ** ‡

Abstract—In this article, a new method to control a flexible robotic arm using a conventional motor with a gear actuator strongly affected by non-linear friction torque is proposed. This control method does not require friction compensation and hence the estimation of this term because the control scheme is robust with respect to this effect. On the other hand, the only variables to measure are the motor shaft and tip angular positions. Velocity measurements, which always introduce errors and noises, are not required. Experimental results are presented.

Keywords: Flexible Robots, GPI control, Flat systems

1 Introduction

In the 1970's flexible robots arise as a new sort of robotic manipulators in engineering. With this new philosophy new applications appeared, most of all in the aerospace industry because lighter robots can be driven in satellites using smaller amounts of energy [1]. Flexible robots are the alternative to rigid robots because of their small weight and high flexibility. Nevertheless, the vibration produced in these flexible structures is difficult to control. Major research effort was made to flexible arms in the 1980's. Several papers appeared on this topic: [2], [3] and [4] are examples of controlling the endpoint position of a flexible robotic arm. In the years 1986 and 1987, Harahima [5], Siciliano et al. [6] used an adaptive control scheme to account for changes in the loads. But in the 1990's the real problems appeared in controlling flexible manipulators with gear reductions coupled in the motor shaft. Researchers had to deal with non linearities such as the friction torque [7]. Robust control schemes with high gain minimized this effect [8]. Compensation of the Coulomb's friction torque accomplished by means of a feed-forward term in the control law was also used in [7]. The most modern technics have been applied to

control flexible arms. Adaptive control [9], sliding control [10] and neural networks [11] are examples of these. But the problem with the friction torque goes on nowadays. In 2006, Cicero *et al.* in [11] used neural networks to compensate this friction effect and explains the necessity of an estimation of this friction model.

In this paper we propose a control method without any friction compensation model. The proposed output feedback control scheme is found to be robust with respect to the effects of the unknown friction torque and no estimation of it is therefore required. Our control scheme is truly an output feedback controller since it only uses the position of the motor and tip. Velocity measurements, which always introduce errors in the signals and noises making it necessary the use of suitable low pass filters sometimes are not required in our control scheme. Becedas *et al.* in [12] in 2006 – 2007, introduced this control method for flexible manipulators. This document is organized as follows: In Section 2 the theoretical model of the flexible manipulator is described. Section 3 is devoted to explain the control method. Section 4 is devoted to show the experimental results obtained with the control scheme applied in a real platform. Finally, the main conclusions of this work are presented in Section 6.

2 Model Description

2.1 Flexible dynamics

A single-link flexible manipulator with tip mass is modeled that can rotate about de Z-axis perpendicular to the paper, as shown in Fig.1. The beam is considered to be an Euler-Bernoulli beam and the axial deformation is neglected, so as to the gravitational effect because the mass of the flexible beam is floating over an air table which allows us to cancel the gravity effect and the friction with the surface of the table. Because structural damping always increases the stability margin of the system, a design without considering damping may provide a valid but conservative result. We study it under the hypothesis of small deformations with all its mass concentrated at the tip position because the mass of the load is bigger than that of the bar, thus the mass of the beam can be neglected. In other words, the flexible beam vibrates with the fundamental mode, therefore the rest of the modes are very far from the first one which can be neglected.

*J. Becedas and V. Feliu are with Universidad de Castilla La Mancha, ETSI Industriales, Av. Camilo José Cela S/N., 13071 Ciudad Real, Spain. Jonathan.Becedas@uclm.es, Vicente.Feliu@uclm.es

†**H. Sira-Ramírez is with Cinvestav IPN, Av. IPN, N°2503, nCol. San Pedro Zacatenco AP 14740, 07300 México, D.F., México. hsira@cinvestav.mx

‡This research was supported by the Junta de Comunidades de Castilla-La Mancha via project ref.:PBI-05-057 and European Social Fund. and by the Spanish Ministerio de Educación y Ciencia via project ref.: DPI2006-13834.

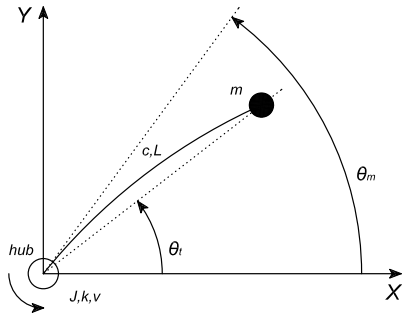


Figure 1: Diagram of a single link flexible arm.

Based on these considerations we propose the following model for the flexible link:

$$mL^2\ddot{\theta}_t = c(\theta_m - \theta_t) \quad (1)$$

where m is the unknown mass in the tip position [kg]. L [m] and $c = \frac{3EI}{L}$ [$N \cdot m$] are the length of the flexible arm and the stiffness of the bar respectively. The stiffness depends on the flexural rigidity EI [$N \cdot m^2$] and on the length of the bar L . θ_m [rad] is the angular position of the motor gear¹. θ_t and $\dot{\theta}_t$ are the unmeasured angular position and angular acceleration [rad/s^2] of the tip respectively.

2.2 Rigid dynamics

A common electromechanical actuator in many control systems is constituted by the DC motor. The DC motor used here is supplied by a servoamplifier with a current inner loop control. We can write the dynamic equation of the system by using Newton's Second law:

$$ku = J\ddot{\theta}_m + \nu\dot{\theta}_m + \hat{\Gamma}_c(\dot{\theta}_m) + \frac{\Gamma}{n} \quad (2)$$

where J is the inertia of the motor [$kg \cdot m^2$], ν is the viscous friction coefficient [$N \cdot m \cdot s$]. $\ddot{\theta}_m$ and $\dot{\theta}_m$ are the angular acceleration of the motor [rad/s^2] and the angular velocity of the motor [rad/s] respectively. $\hat{\Gamma}_c$ is the unknown Coulomb friction torque which affects the motor dynamics [$N \cdot m$]. This nonlinear friction term is considered as a perturbation, depending only on the sign of the motor angular velocity. As a consequence, Coulomb's friction, when $\dot{\theta}_m \neq 0$, follows the model:

$$\hat{\Gamma}_c \cdot \text{sign}(\dot{\theta}_m) = \begin{cases} \hat{\Gamma}_c (\dot{\theta}_m > 0) \\ -\hat{\Gamma}_c (\dot{\theta}_m < 0) \end{cases} \quad (3)$$

and, when $\dot{\theta}_m \approx 0$ the dynamics is similar to that on (3) but, in this case, depending on the sign of the voltage u . The parameter k is the known electromechanical constant of the motor servo-amplifier system [Nm/V]. Γ is the

¹We denote by n the reduction ratio of the motor gear, thus $\theta_m = \hat{\theta}_m/n$ where $\hat{\theta}_m$ is motor shaft position.

coupling torque measured in the hub [$N \cdot m$] and n is the reduction ratio of the motor gear. u is the motor input voltage [V]. This variable is the control variable of the system. This is the input to a servo-amplifier which controls the input current to the motor by means of an internally PI current controller. This electrical dynamics can be rejected because this is faster than the mechanical dynamics of the motor. Thus, the servo-amplifier can be considered as a constant relation between the voltage and the current to the motor.

2.3 System

The dynamics of the complete system, actuated by a DC motor is given by the following simplified model:

$$mL^2\ddot{\theta}_t = c(\theta_m - \theta_t) \quad (4)$$

$$ku = J\ddot{\theta}_m + \nu\dot{\theta}_m + \hat{\Gamma}_c + \frac{\Gamma}{n} \quad (5)$$

$$\Gamma = c(\theta_m - \theta_t) \quad (6)$$

Equation (4) represents the dynamics of the flexible beam, equation (5) represents the dynamics of the DC motor and equation (6) represents the coupling torque measured in the hub and produced by the translation of the flexible beam, which is directly proportional to the stiffness of the beam and the difference between the positions of the motor and the tip respectively.

3 Generalized proportional integrator controller

In Laplace transforms notation, the flexible bar transfer function, obtained from (4), can be written as follows,

$$Gb(s) = \frac{\theta_t(s)}{\theta_m(s)} = \frac{\omega_0^2}{s^2 + \omega_0^2} \quad (7)$$

where $\omega_0 = (c/(mL^2))^{1/2}$ is the unknown natural frequency of the bar due to the lack of precise knowledge of m . The coupling torque can be canceled in the motor by means of a compensation term. In this case the voltage applied to the motor is of the form,

$$u = u_c + \frac{\Gamma}{k \cdot n} \quad (8)$$

where u_c is the voltage applied before the compensation term. The system in (5) is then given by:

$$ku_c = J\ddot{\theta}_m + \nu\dot{\theta}_m + \hat{\Gamma}_c \quad (9)$$

The controller to be designed will be robust with respect to the unknown piecewise constant torque disturbances affecting the motor dynamics, $\hat{\Gamma}_c$. Then the perturbation free system to be considered is the following:

$$Ku_c = J\ddot{\theta}_m + \nu\dot{\theta}_m \quad (10)$$

Where $K = k/n$. To simplify the developments, let $A = K/J$, $B = \nu/J$. The DC motor transfer function is then written as:

$$G_m(s) = \frac{\theta_m(s)}{u_c(s)} = \frac{A}{s(s+B)} \quad (11)$$

Fig.2 depicts the compensation scheme of the coupling torque measured in the hub. The regulation of the load

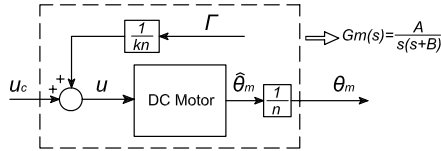


Figure 2: Compensation of the coupling torque measured in the hub

position $\theta_t(t)$ to track a given smooth reference trajectory, $\theta_t^*(t)$, is desired. For the synthesis of the feedback law we are using only the measured motor position θ_m and the measured coupling torque Γ .

3.1 Outer loop controller

Consider the model of the flexible link, given in (4). This subsystem is flat, with flat output given by θ_t (See [13]). The parametrization of θ_m in terms of θ_t is given, in reduction gear terms, by:

$$\theta_m = \frac{mL^2}{c} \ddot{\theta}_t + \theta_t = \frac{1}{\omega_0^2} \ddot{\theta}_t + \theta_t \quad (12)$$

System (12) is a second order system in which to regulate the tip position of the flexible bar, θ_t , towards a given smooth reference trajectory $\theta_t^*(t)$ is desired, with θ_m acting as an *auxiliary* control input. Clearly, if there exists an auxiliary open loop control input, $\theta_m^*(t)$, that ideally achieves the tracking of $\theta_t^*(t)$ for suitable initial conditions, it satisfies then the second order dynamics, in reduction gear terms (13).

$$\theta_m^*(t) = \frac{1}{\omega_0^2} \ddot{\theta}_t^*(t) + \theta_t^*(t) \quad (13)$$

Subtracting (13) from (12), an expression in terms of the angular tracking errors is obtained:

$$\ddot{e}_{\theta_t} = \omega_0^2 (e_{\theta_m} - e_{\theta_t}) \quad (14)$$

where $e_{\theta_m} = \theta_m - \theta_m^*(t)$, $e_{\theta_t} = \theta_t - \theta_t^*(t)$. Suppose for a moment we are able to measure the angular position tracking error, e_{θ_t} , then the outer loop feedback incremental controller could be proposed to be the following PID controller,

$$e_{\theta_m} = e_{\theta_t} + \frac{1}{\omega_0^2} \left[-k_2 \dot{e}_{\theta_t} - k_1 e_{\theta_t} - k_0 \int_0^t e_{\theta_t}(\sigma) d\sigma \right] \quad (15)$$

In such a case, the closed loop tracking error e_{θ_t} evolves governed by,

$$e_{\theta_t}^{(3)} + k_2 \ddot{e}_{\theta_t} + k_1 \dot{e}_{\theta_t} + k_0 e_{\theta_t} = 0 \quad (16)$$

The design parameters $\{k_2, k_1, k_0\}$, are then chosen so as to render the closed loop characteristic polynomial, into a Hurwitz polynomial with desirable roots. However, in order to avoid tracking error velocity measurements, we propose to obtain an *integral reconstructor* for the angular velocity error signal \dot{e}_{θ_t} . We proceed by integrating the expression (14) once; and, later, by disregarding the constant error due to the tracking error velocity initial conditions. The estimated error velocity $[\dot{e}_{\theta_t}]_e$ can be computed in the following form:

$$[\dot{e}_{\theta_t}]_e = \dot{e}_{\theta_t}(t) - \dot{e}_{\theta_t}(0) = \omega_0^2 \int_0^t (e_{\theta_m}(\sigma) - e_{\theta_t}(\sigma)) d\sigma \quad (17)$$

The integral reconstructor neglects the possibly nonzero initial condition $\dot{e}_{\theta_t}(0)$ and, hence, it exhibits a constant estimation error. When the reconstructor is used in the derivative part of the PID controller, the constant error is suitably compensated thanks to the integral control action of the PID controller. Substituting the integral reconstructor $[\dot{e}_{\theta_t}]_e$ (17) by \dot{e}_{θ_t} into the PID controller (15) and after some rearrangements we obtain:

$$(\theta_m - \theta_m^*) = \left[\frac{\gamma_1 s + \gamma_0}{s + \gamma_2} \right] (\theta_t^* - \theta_t) \quad (18)$$

The tip angular position can not be measured, but it certainly can be computed from the expression relating the tip position with the motor position and the coupling torque (Γ):

$$\Gamma = c(\theta_m - \theta_t) = mL^2 \ddot{\theta}_t \quad (19)$$

Thus, the angular position θ_t is readily expressed as,

$$\theta_t = \theta_m - \frac{1}{c} \Gamma \quad (20)$$

Fig. 3 depicts the feedback outer loop control scheme. This is exponentially stable. To specify the parameters, $\{\gamma_2, \gamma_1, \gamma_0\}$, we can choose to locate the closed loop poles in the left half of the complex plane. All three poles can be located in the same point of the real line, $s = -a$, a being strictly positive, using the following polynomial equation,

$$(s + a)^3 = s^3 + 3as^2 + 3a^2s + a^3 = 0 \quad (21)$$

Where the parameter a represents the desired location of the poles. The characteristic equation of the closed loop system is,

$$s^3 + \gamma_2 s^2 + \omega_0^2(1 + \gamma_1)s + \omega_0^2(\gamma_2 + \gamma_0) = 0 \quad (22)$$

Identifying each term of the expression (21) with those of (22), the design parameters $\{\gamma_2, \gamma_1, \gamma_0\}$ can be uniquely specified if ω_0 is known.

3.2 Inner loop controller

The angular position θ_m , generated as an auxiliary control input in the previous controller design step, is now regarded as a reference trajectory for the motor controller. We denote this reference trajectory by θ_{mr}^* . The dynamics of the DC motor, including the Coulomb friction term, is given by (9). The design of the controller to be robust with respect to this torque disturbance is desired. The following feedback controller is proposed,

$$e_\nu = \frac{\nu}{K} [\dot{e}_{\theta_m}]_e + \frac{J}{K} [-k_3 [\dot{e}_{\theta_m}]_e - k_2 e_{\theta_m} - k_1 \int_0^t e_{\theta_m}(\sigma) d\sigma - k_0 \int_0^t \int_0^{\sigma_1} (e_{\theta_m}(\sigma_2)) d\sigma_2 d\sigma_1] \quad (23)$$

The following *integral reconstructor* for the angular velocity error signal $[\dot{e}_{\theta_m}]_e$ is obtained.

$$[\dot{e}_{\theta_m}]_e = \frac{K}{J} \int_0^t e_\nu(\sigma) d\sigma - \frac{\nu}{J} e_{\theta_m} \quad (24)$$

Replacing $[\dot{e}_{\theta_m}]_e$ (24) into (23) and after some rearrangements the feedback control law is obtained as:

$$(u_c - u_c^*) = \left[\frac{\alpha_2 s^2 + \alpha_1 s + \alpha_0}{s(s + \alpha_3)} \right] (\theta_{mr}^* - \theta_m) \quad (25)$$

The open loop control $u_c^*(t)$ that ideally achieves the open loop tracking of the inner loop is given by

$$u_c^*(t) = A^{-1} \ddot{\theta}_m^*(t) + BA^{-1} \dot{\theta}_m^*(t) \quad (26)$$

The inner loop system in Fig. 3 is exponentially stable. We can choose to place the closed loop poles in a desired location of the left half of the complex plane in order to design the parameters $\{\alpha_3, \alpha_2, \alpha_1, \alpha_0\}$. As done with the outer loop, all poles can be located at the same real value and $\alpha_3, \alpha_2, \alpha_1$ and α_0 can be uniquely obtained equalizing the terms of the two following polynomials:

$$(s + p)^4 = s^4 + 4ps^3 + 6p^2s^2 + 4p^3s + p^4 = 0 \quad (27)$$

$$s^4 + (\alpha_3 + B)s^3 + (\alpha_3B + \alpha_2A)s^2 + \alpha_1As + \alpha_0A = 0 \quad (28)$$

where the parameter p represents the common location of all the closed loop poles, this being strictly positive. Fig. 3 depicts the closed loop control system under which the outer and inner loop are implemented in practise.

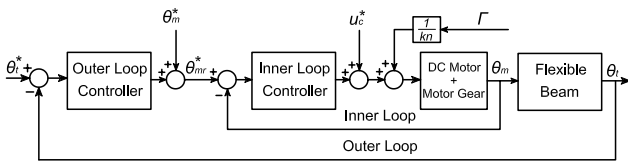


Figure 3: Flexible link dc motor system controlled by a two stage GPI controller design.

4 Experimental Validation

This section is devoted to experimentally validate the previous algorithm.

4.1 Experimental Setup Description

Fig.4(a) depicts a picture of the used experimental platform constituted by a three legged metallic structure to support an Harmonic Drive mini servo DC motor RH-8D-6006-E036AL-SP(N) which has a reduction ratio characterized by $n = 50$. The frame makes possible the stably and free rotation of the motor in the horizontal plane around the vertical axis of the platform. The parameter values are: inertia $J = 6.87 \cdot 10^{-5} [kg \cdot m^2]$, viscous friction $\nu = 1.041 \cdot 10^{-3} [N \cdot m \cdot s]$ and electromechanical constant $k = 0.21 [N \cdot m/V]$. With these parameters, A and B of the transfer function of the DC motor in (11) can be computed as: $A = 61.14 [N/(V \cdot kg \cdot s)]$, $B = 15.15 [N \cdot s/(kg \cdot m)]$. The servoamplifier accepts control inputs from the computer in the range of $[-10, 10] [V]$. The flexible bar is attached to the motor. The load floats over the surface of an air table, so the gravity effect and the friction of the load with the surface of the table are canceled. The values of the flexible beam parameters are: the length $L = 0.5 [m]$ and diameter $d = 3 \cdot 10^{-3} [m]$. The flexural rigidity of the bar is $EI = 0.260 [N \cdot m^2]$, therefore the stiffness is $c = 1.585 [N \cdot m]$. The tip load parameters is a wood disc with mass $m = 3 \cdot 10^{-2} [kg]$. With these parameters, the natural frequency of the bar characterized in transfer function (7) can be computed as: $\omega_0 = 14.54 [rad/s]$. The sensor system is integrated by an encoder embedded in the motor which allows us to know the motor position with a precision of $7 \cdot 10^{-5} [rad]$. And a pair of strain gauges with gage factor 2.16 and resistance $120.2 [\Omega]$. The sample time in the signals processing is $2 [ms]$. In order to obtain the natural frequency of the system ω_0 to validate the one mode model proposed, a torque in the motor shaft was applied. Then the tip of the beam oscillated. The oscillation is translated as a peak in the periodogram² (see Fig. 4(b)). The estimation provided by the peak of the periodogram, observed at the abscissa axis is $f_0 \approx 2.4 [Hz]$, this is $\omega_0 \approx 2.4 \cdot 2\pi \approx 15.1 [rad/s]$. Note that in the periodogram only clearly appears one noticeable mode.

4.2 Outer loop design

We locate the poles of the outer loop at -12 in the real axis, thus we assure that the inner loop is faster than the outer one. The transfer function of the controller is given by the following expression:

$$\frac{\theta_m - \theta_m^*}{\theta_t^* - \theta_t} = \frac{1.044s - 27.82}{s + 36} \quad (29)$$

²Recall that the periodogram of the signal $u(t)$, $t = 1, 2, \dots, N$ is $|U_N(\omega)|^2$, where $U_N(\omega) = \frac{1}{\sqrt{N}} \sum_{t=1}^N U_N(2\pi k/N) e^{i2\pi kt/N}$, $k = 1, \dots, N$ represents the discrete Fourier's transform (DFT) for $\omega = 2\pi k/N$

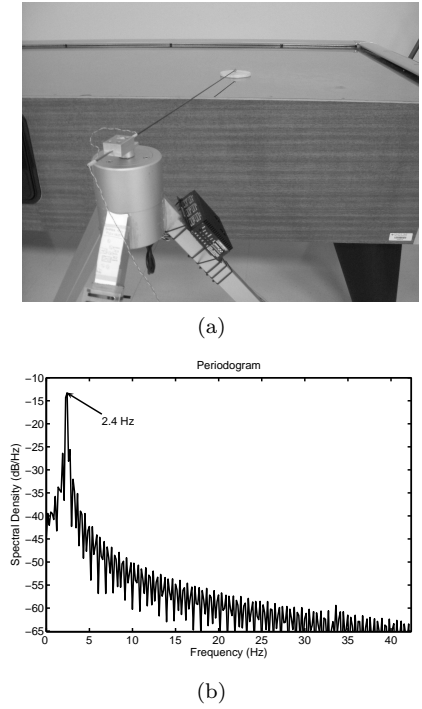


Figure 4: (a) Photograph of the flexible arm platform. (b) Periodogram of the flexible beam oscillation.

The open loop reference control input $\theta_m^*(t)$ in (13) is given by,

$$\theta_m^*(t) = 4.7 \cdot 10^{-3} \ddot{\theta}_t^*(t) + \theta_t^*(t) \quad (30)$$

$\theta_t^*(t)$ being the desired (rest-to-rest) reference trajectory of the angular displacement of the arm tip.

4.3 Inner loop design

Closed loop poles are placed at -110 . Then the transfer function of the controller results:

$$\frac{u_c - u_c^*}{\theta_m^* - \theta_m} = \frac{1.08 \cdot 10^3 s^2 + 8.71 \cdot 10^4 s + 2.40 \cdot 10^6}{s(s + 424.85)} \quad (31)$$

The feed-forward term in (26) is computed according to,

$$u_c^*(t) = 16.4 \cdot 10^{-3} \ddot{\theta}_m^*(t) + 0.25 \ddot{\theta}_m^*(t) \quad (32)$$

5 Experimental results

Fig.5(a) shows the commanded trajectory (θ_t^*) and the response of the closed loop system (θ_t) which is here compared with that of the simulations (such a response is here denoted by θ_{ts}). Note that the experimental response θ_t perfectly tracks the reference trajectory as done in simulations; all signals are superimposed. Fig.5(b) depicts a zoom of the tip position of the flexible arm at the beginning of the trajectory. Note that the tip position precisely follows the simulated response θ_{ts} and the error with respect the reference is almost insignificant. Fig.5(c)

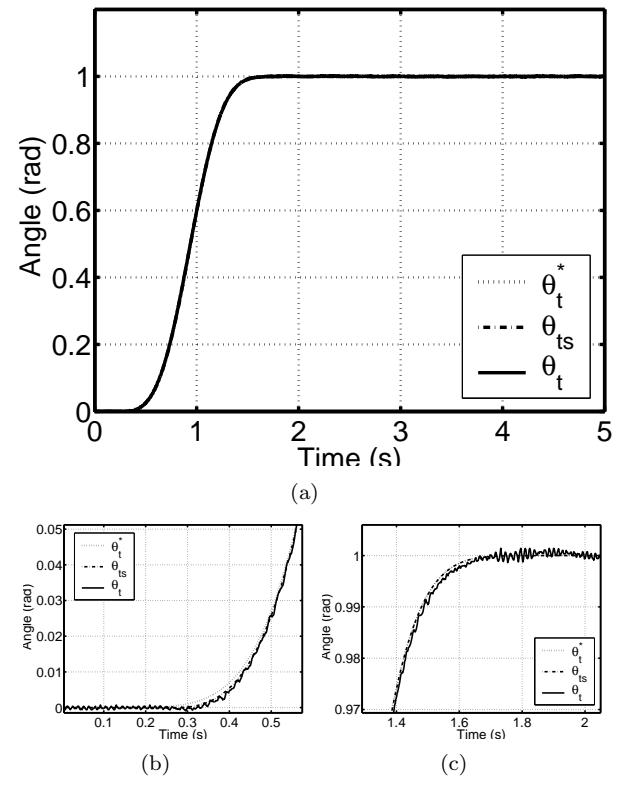


Figure 5: Experimental tip position trajectory tracking. (a) Zoom at the beginning of the trajectory. (b) Zoom at the end of the trajectory.

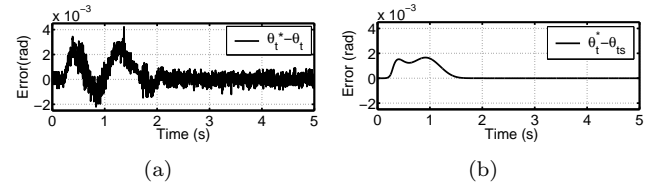


Figure 6: Trajectory tracking error. (a) Experimental. (b) Simulated.

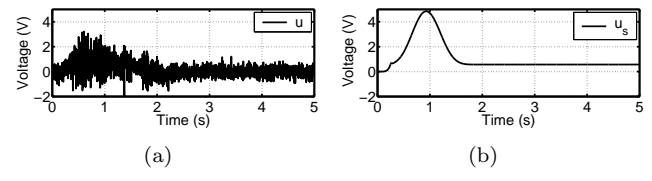


Figure 7: Control voltage to the DC motor. (a) Experimental. (b) Simulated.

depicts a zoom of the system trajectory tracking at the end of the trajectory. There not appears overshoot in the experimental tracking so as to the simulated one. The error is minimized when the system reaches the steady state. Fig.6(a) depicts how the trajectory tracking error rapidly converges to zero, and thus a quite precise tracking of the desired trajectory is achieved. The experimental error can be compared with the simulated one Fig.6(b). The experimental error is corresponded with the previewed in simulations. Fig.7(a) depicts the experimental input voltage to the DC motor u . Note that this signal never reaches values which saturate the amplifier (i.e $+10V$, $-10V$). We can compare this signal with that of the simulations (see Fig.7(b)) and observe that the two signals are similar in shape. Obviously the experimental signal is noisier because of the real behavior of the physical platform. In Fig.8(a) the experimental tra-

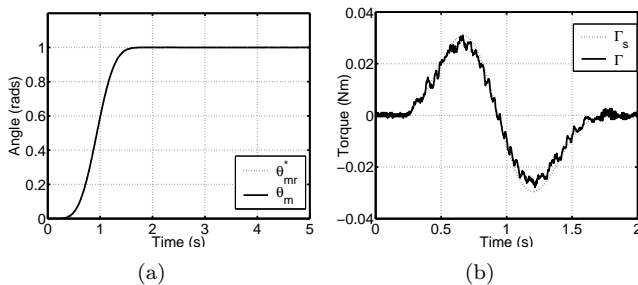


Figure 8: (a) Experimental motor position tracking. (b) Coupling torque measured by the strain gauges.

jectory tracking of the DC motor is presented. Although, the objective of the controller is to control the tip position of the flexible beam this picture shows that the inner loop has a good tracking performance. Fig.8(b) depicts the coupling torque produced in the hub Γ . This signal is compared with the simulated coupling torque Γ_s . Although the experimental coupling torque is noisier than the simulated one, we can observe that the two signals are similar, they have the same phase and amplitude.

6 CONCLUSIONS

A two stage *GPI* controller design scheme has been proposed for the regulation and reference trajectory tracking of a single-link flexible arm. The *GPI* control scheme here proposed only requires the measurement of the angular position of the motor and that of the tip velocity measurements which always introduce noises and errors are not required. On the other hand the controller proposed is found to be robust with respect nonlinear friction effects. Therefore, estimation of these is not required.

References

[1] Maizza-Neto O., "Modal analysis and control of flexible manipulator arms", *Ph. D. dissertation, Dept.*

Mech. Eng, MIT, Cambridge, 1974.

- [2] Schmitz E., "Experiments on the end-point control of a very flexible one-link manipulator", *Ph. D. dissertation, Dept. Aeronaut. Astronaut., Stanford University, 1985.*
- [3] Cannon R. H. and Schmitz E., "Precise control of flexible manipulators", *Robotic Research, 1985.*
- [4] Matsuno F., Fukushima F. and coworkers., "Feedback control of a flexible manipulator with a parallel drive mechanism", *Int. J. Robotics Research, V6, N4, 1987.*
- [5] Harahima F. and Ueshiba T., "Adaptative control of flexible arm using end-point position sensing", *Japan-USA Symp. Flexible Automation, 1986.*
- [6] Siciliano B., Yuan B. S. and Book W. J., "Model reference adaptative control of a one link flexible arm", *IEEE Conf Decision and Contr, Athens, Greece, 1986.*
- [7] Olsson H., Amström K.J and Canudas de Wit C., "Friction Models and friction Compensation", *European Journal of Control, V4, pp. 176-195, 1998.*
- [8] Feliu V., Rattan K.S. and Brown H.B., "Control of flexible arms with friction in the joints", *IEEE Trans. on Robotics and Automation, V9, N4, pp. 467-475, 1993.*
- [9] Yang T.C., Yang J.C.S. and Kudva P., "Load adaptative control of a single-link flexible manipulator", *IEEE Trans Syst Man Cybernet, V22, N1, pp. 85-91, 1992.*
- [10] Chen Y. and Hsu H., "Regulation and vibration control of a FEM-based single-link flexible arm using sliding-mode theory", *J. Vibrat Control, V7, N5, pp. 741-52, 2001.*
- [11] Cícero S., Santos V. and de Carvahlo B., "Active Control to flexible manipulators", *IEEE/ASME Transactions on Mechatronics, V11, N1, pp. 75-83, 2006.*
- [12] Becedas J., Trapero J. R., Sira-Ramírez H. and Feliu V., "Fast identification method to control a flexible manipulator with parameters uncertainties", *IEEE International Conference on Robotics and Automation, 2007.*
- [13] Sira-Ramírez H. and Agrawal S., *Differentially Flat Systems*, Marcel Dekker, 2004.